Research Article Vol. 11, No. 12 / December 2023 / Photonics Research 2179

PHOTONICS Research

Optomechanical feedback cooling of a 5 mm long torsional mode

Dianqiang Su,[1,2] Yuan Jiang,[1,2] Pablo Solano,[3,4] Luis A. Orozco,[5] John Lawall,[6] and Yanting Zhao[1,2,*]

[1]State Key Laboratory of Quantum Optics and Quantum Optics Devices, Institute of Laser Spectroscopy, Shanxi University, Taiyuan 030006, China
[2]Collaborative Innovation Center of Extreme Optics, Shanxi University, Taiyuan 030006, China
[3]Departamento de Física, Facultad de Ciencias Físicas y Matemáticas, Universidad de Concepción, Concepción, Chile
[4]CIFAR Azrieli Global Scholars Program, CIFAR, Toronto, Ontario M5G 1M1, Canada
[5]Joint Quantum Institute, Department of Physics and NIST, University of Maryland, College Park, Maryland 20742, USA
[6]National Institute of Standards and Technology, Gaithersburg, Maryland 20899, USA
*Corresponding author: zhaoyt@sxu.edu.cn

Received 6 February 2023; revised 10 September 2023; accepted 11 October 2023; posted 11 October 2023 (Doc. ID 487035); published 30 November 2023

We report three orders of magnitude optical cooling of the fundamental torsional mode of a 5 mm long, 550 nm diameter optical nanofiber. The rotation of the nanofiber couples to the polarization of guided laser fields. We use a weak laser probe to monitor the rotation and use feedback to modulate the polarization of an auxiliary drive laser providing torque. Our results present a tool for the optomechanical control of large-scale torsional resonators, with metrological applications and potential implications for studying macroscopic objects in quantum states.

https://doi.org/10.1364/PRJ.487035

1. INTRODUCTION

Optomechanics uses light to monitor and control the motion of micro- and macroscale objects [1]. State-of-the-art optical cooling has reached the quantum ground state of translational motion in a number of platforms [2–10], an essential step for fundamental tests of quantum mechanics on massive objects [11–13]. In such a context, larger and more massive systems will enable us to test the limits of current theories [14–17]. Moreover, precise control and transduction of mechanical motion enables metrological applications [18]. Controlling rotational degrees of freedom, however, remains challenging [19], in part because rotation does not couple naturally to an optical cavity.

In this work, we report purely optical feedback cooling [1,20–24] of a 5 mm long torsional resonator with a frequency of ≈190 kHz, reducing the mean-square angular displacement over three orders of magnitude from room temperature. The platform is the fundamental torsional mode of an optical nanofiber (ONF), coupled to the polarization of the guided light [25–27]. We perform in-loop and out-of-loop measurements and observe cooling from the reduction of the angular fluctuations and broadening of the spectral density of the fluctuations. The measured optimal cooling is near the theoretical limit of the technique given by the signal-to-noise ratio (SNR) [28,29], scaling as $\sim 2\sqrt{1/\mathrm{SNR}} \approx 1.2 \times 10^{-3}$. Moreover, the platform presents a torque sensitivity $\approx 10^{-26}$ N m Hz$^{-1/2}$, comparable with the record sensitivities achieved with nanodumbells [30]. Our results demonstrate ONFs to be a fruitful platform for rotational optomechanics, with potential applications in metrology and quantum optomechanics.

2. THEORETICAL MODEL

The ONF is a silica cylinder of diameter ≈550 nm and length ≈5 mm created by tapering a length of standard optical fiber, as shown in Fig. 1(b). It has string, compressional, and torsional modes [31], the latter of which couples to the polarization of guided light due to intrinsic birefringence produced during the fabrication process. When linearly polarized light of power P_{opt} propagates through the fiber, it results in an optically induced torque $\tau_{\mathrm{opt}} = \tau_0 P_{\mathrm{opt}} \sin(2(\theta - \theta_L))$, where τ_0 has units of torque per unit power, θ is the angle of the slow axis, and θ_{L} is the angle of the polarization [27,32].

A fluctuating Langevin torque τ_{th} with white spectral density and an external torque from applied optical feedback drive the ONF. The equation of motion for the angular coordinate θ representing the slow axis of the fundamental torsional mode is

$$I\ddot{\theta} + \gamma\dot{\theta} + \kappa\theta = \tau_{\mathrm{th}} + \tau_0 P_{\mathrm{opt}} \sin(2(\theta - \theta_L)), \quad (1)$$

where I is the effective moment of inertia of the mode, γ is the damping coefficient, and κ is the torsional spring constant. τ_{th} is the thermally induced torque with a double-sided power spectral density $S_{\tau_{\mathrm{th}}} = 2\gamma k_B T$, where T is the temperature

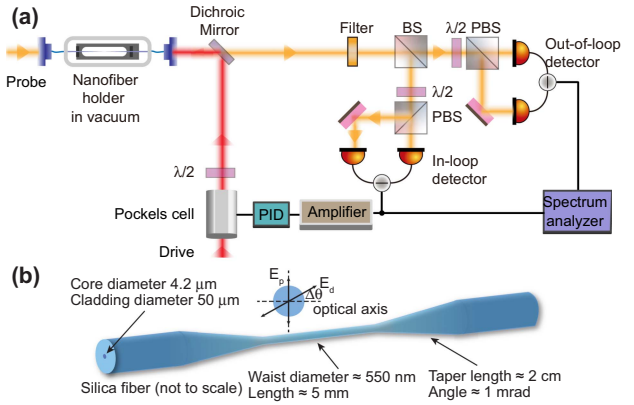

Fig. 1. (a) Apparatus schematic. Probe and drive laser beams counterpropagate with independent polarization control. A beam splitter (BS) separates the probe into out-of-loop and in-loop detection. Each path has a half-wave plate ($\lambda/2$) to set the detection basis, followed by a polarizing beam splitter (PBS) and a balanced photodiode pair. The out-of-loop detection signal goes to a spectrum analyzer, while the in-loop signal splits parts, one to the spectrum analyzer, and the other is amplified, filtered (≈100 kHz wide centered on resonance), and then goes to a control unit that slightly rotates the drive polarization closing the feedback loop. (b) ONF schematic with two effective polarization axes: ordinary and extraordinary indices of refraction, aligned with the optical axes but at an angle $\Delta\theta$ with the input light polarization. The fiber is clamped (not shown) in the unmodified section.

and k_B is the Boltzmann constant. In the absence of optically applied torque ($P_{\mathrm{opt}} = 0$), the system comes to thermal equilibrium with $\langle\theta^2\rangle = k_B T/\kappa \approx 10^{-8}$ rad^2.

When a static optical field is introduced, the torque results in a new equilibrium angle $\bar{\theta}$, found by dropping the time derivatives and fluctuating torque τ_{th} in Eq. (1), yielding the transcendental equation $\kappa\bar{\theta} = \tau_0 P_{\mathrm{opt}} \sin(2(\bar{\theta} - \theta_L))$. Feedback will be introduced by modulating the polarization angle θ_L with a Pockels cell. Taking $\theta_L = \bar{\theta}_L + \delta\theta_L$ and $\theta = \bar{\theta} + \delta\theta$ and linearizing Eq. (1) about the steady-state, one obtains

$$I\delta\ddot{\theta} + \gamma\delta\dot{\theta} + \kappa\delta\theta = \tau_{\mathrm{th}} + 2\beta\tau_0 P_{\mathrm{opt}}(\delta\theta - \delta\theta_L), \tag{2}$$

where we define $\beta = \cos(2(\bar{\theta} - \bar{\theta}_L))$. Taking the Fourier transform, we find

$$\left(-\omega^2 + i\omega\Gamma + \omega_m^2 - \frac{2\beta P_{\mathrm{opt}}}{I}\tau_0[\omega]\right)\delta\theta[\omega] = \frac{1}{I}(\tau_{\mathrm{th}}[\omega] - 2\beta P_{\mathrm{opt}}\tau_0[\omega]\delta\theta_L[\omega]), \tag{3}$$

where $\Gamma = \gamma/I$ and $\omega_m^2 = \kappa/I$; we have also allowed for frequency dependence in $\tau_0[\omega]$. In previous work [27], we demonstrated that the intrinsic delay in the response of the torque to changes in θ_L, arising from the finite speed of sound, led to self-cooling with fixed optical drive ($\delta\theta_L = 0$). However, such a passive feedback scheme is limited because it does not allow controlling the feedback gain or phase. Although Ref. [27] sets the working principles of the platform, the temperature reduction permitted by self-cooling was limited to a factor of 5. These results suggest that active feedback is necessary to improve the cooling performance.

Here, we use active feedback such that $\delta\theta_L[\omega] = G[\omega]\delta\theta[\omega]$, where $G[\omega]$ describes the collective transfer function of the balanced photodetector, amplifier, proportional integral derivative controller, and Pockels cell shown in Fig. 1. In practice, there will always be measurement noise θ_n to which the feedback will respond as well; taking $\delta\theta[\omega] \to \delta\theta[\omega] + \theta_n[\omega]$, we find

$$\left(-\omega^2 + i\omega\Gamma + \omega_m^2 - \frac{2\beta}{I}P_{\mathrm{opt}}\tau_0[\omega](1 + G[\omega])\right)\delta\theta[\omega] = \frac{1}{I}(\tau_{\mathrm{th}}[\omega] - 2\beta P_{\mathrm{opt}}\tau_0[\omega]G[\omega]\theta_n[\omega]). \tag{4}$$

The term proportional to P_{opt} on the left-hand side of Eq. (4) can be chosen, by means of $G[\omega]$, to maintain the form of a harmonic oscillator while altering its damping rate and/or natural frequency. Neglecting the frequency dependence of τ_0, we choose derivative feedback with transfer function $G[\omega] = i\omega G_D$ in order to add a term (proportional to $i\omega$) corresponding to damping. Equation (4) then takes the form of a harmonic oscillator with optically modified damping rate $\Gamma' = \Gamma - \frac{2\beta}{I}P_{\mathrm{opt}}\tau_0 G_D$, frequency $\omega_m' = (\omega_m^2 - \frac{2\beta}{I}P_{\mathrm{opt}}\tau_0)^{1/2}$, and torsional spring constant $\kappa' = I\omega_m'^2$ driven by fluctuations with torque spectral density

$$S_\tau = 2I\Gamma k_B T + 4\beta^2 P_{\mathrm{opt}}^2\tau_0^2 G_D^2\omega^2 S_{\theta_n}[\omega], \tag{5}$$

where S_{θ_n} is the spectral density of the measurement noise, and T is the ambient temperature. By adding a proportional gain term so that $G[\omega] = G_P + i\omega G_D$, it is possible to modify the frequency of the oscillator as well as the damping, but this would come at the expense of an additional noise term on the right-hand side of Eq. (4).

The spectral density of the angular fluctuations is then given by

$$S_{\delta\theta} = \frac{1}{I^2}\frac{2I\Gamma k_B T + 4S_{\theta_n}[\omega]\beta^2 P_{\mathrm{opt}}^2\tau_0^2 G_D^2\omega^2}{(\omega_m'^2 - \omega^2)^2 + \omega^2\Gamma'^2}. \tag{6}$$

Integration over all frequencies yields the mean-square angular fluctuations. Assuming a white spectral density for the measurement noise, the integral can be evaluated analytically:

$$\langle\delta\theta^2\rangle = \frac{1}{2\pi}\int_{-\infty}^{\infty} S_{\delta\theta}\mathrm{d}\omega = \frac{k_B T}{\kappa'}\frac{\Gamma}{\Gamma'} + \frac{2\beta^2 P_{\mathrm{opt}}^2\tau_0^2 G_D^2}{I^2\Gamma'}S_{\theta_n}. \tag{7}$$

Defining an effective mode temperature by $k_B T_{\mathrm{mode}} = I\omega_m'^2\langle\delta\theta^2\rangle$ and a dimensionless feedback gain $g = -\frac{2\beta}{I\Gamma}P_{\mathrm{opt}}\tau_0 G_D$, one finds

$$\frac{T_{\mathrm{mode}}}{T} = \frac{1}{1+g}\left(1 + g^2\frac{S_{\theta_n}}{S_s}\right), \tag{8}$$

where $S_s = 2k_B T/\Gamma I\omega_m'^2$ is the on-resonance spectral density of the angular fluctuations in Eq. (6) in the absence of feedback. The dimensionless gain g can be varied by means of the polarization angle $\bar{\theta}_L$ (via β), optical power, or electronic gain. By differentiating Eq. (8), one finds that, for a given SNR S_s/S_{θ_n}, the mode temperature is minimized for $g_{\mathrm{opt}} = \sqrt{1 + S_s/S_{\theta_n}} - 1$. In the limit of large SNR, $g_{\mathrm{opt}} \to \sqrt{S_s/S_{\theta_n}}$ and

$$\frac{T_{\mathrm{mode}}}{T} \to \frac{2}{\sqrt{S_s/S_{\theta_n}}}. \tag{9}$$

The torsional mode cooling will continue as long as the in-loop measurement can resolve the signal of torsional motion from the noise. Hence, the relative temperature reduction depends only on the SNR, the crucial figure of merit for feedback cooling, and it is manifestly independent of T, as shown in Eq. (9).

The reduction of the mode temperature can be measured in various ways. For high Q systems, even in the presence of feedback, it is given by $k_B T_{\mathrm{mode}} = I\omega_{\mathrm{m}}'^2\langle\delta\theta^2\rangle$, where $\langle\delta\theta^2\rangle$ is determined in terms of the integral of the measured distribution $S_{\delta\theta}$. It is also related to the broadened linewidth Γ' of $S_{\delta\theta}$ by

$$\frac{T_{\mathrm{mode}}}{T} = \frac{\Gamma}{\Gamma'}\left(1 + \frac{(\Gamma'/\Gamma - 1)^2}{\mathrm{SNR}}\right), \tag{10}$$

so that the cooling scales inversely with the linewidth of the angular spectral density as long as the linewidth broadening is not too great; for large enough values of the feedback, the linewidth will continue to broaden, but the mode temperature will rise. Finally, the squared fluctuating amplitude $\delta\theta^2(t)$ of the torsional oscillation can be measured in the time domain, and the statistics of a long series of measurements will follow a Boltzmann distribution:

$$p(\delta\theta^2) = \frac{\kappa'}{2k_B T_{\mathrm{mode}}} e^{-\kappa'\delta\theta^2/(2k_B T_{\mathrm{mode}})}, \tag{11}$$

from which T_{mode} can be extracted.

3. EXPERIMENTAL SETUP

Figure 1 shows the experimental apparatus. We heat and pull [33] a commercial optical fiber (50 μm cladding, 4.2 μm core) to produce a ≈550 nm diameter, ≈5 mm length waist with a ≈1 mrad taper. For the wavelengths used, it allows the propagation of the fundamental HE_{11} mode [34]. The nanofiber resides in a vacuum chamber at a pressure of 10^{-5} Pa (10^{-7} mbar) to suppress air damping; Ref. [25] shows that the Q saturates at a pressure $P < 10^{-2}$ Pa (10^{-4} mbar). The fundamental torsional resonance of the ONF is at about 190 kHz with a half width at half maximum of 0.75(5) Hz, corresponding to a mechanical quality factor $Q \approx 1.26(8) \times 10^5$. All the uncertainties reported in the text and Figs. 2 and 3 correspond to one standard deviation as obtained using the χ^2 method of the fits.

In order to measure the angular fluctuations of the ONF, 250 μW of linearly polarized probe laser light at 852 nm is coupled in, and the transmitted polarization is redundantly analyzed by two pairs of balanced photodetectors (BPDs). Rotation of the ONF causes a linear rotation of the output polarization due to the ONF birefringence, and the balanced detection scheme provides a signal proportional to $\delta\theta$ while removing common-mode laser intensity fluctuations. One BPD is used as an "in-loop" detector for feedback; the other is used for "out-of-loop" detection. The signal from either BPD can be sent to a spectrum analyzer, used either to observe the spectral density of the signal, or in zero-span mode as a fixed programmable bandpass filter to eliminate technical noise in a measurement of the squared angular fluctuations $\delta\theta^2(t)$ as a function of time. Calibration is accomplished by assuming that the observed fluctuations in the absence of feedback are of thermal origin at room temperature. Feedback is applied by means of a linearly polarized "drive" laser [Fig. 1(a)] whose polarization angle θ_L is controlled by a Pockels cell, generating torque on the ONF. The output of one of the "in-loop" BPD is amplified and filtered to produce a signal corresponding approximately to derivative feedback and then applied to the Pockels cell. The loop gain can be controlled by means of the mean polarization $\bar{\theta}_L$, drive laser power, or electronic gain. We observe similar results in each case but vary the drive laser power in this work.

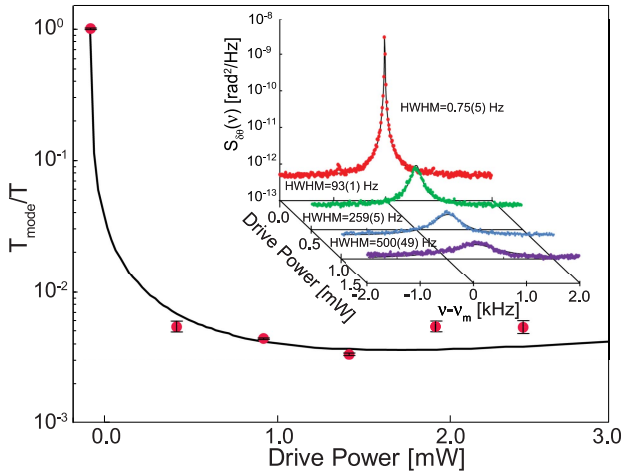

Fig. 2. Mode temperature, calculated from the integral of $S_{\delta\theta}(\omega)$ from out-of-loop measurements, as a function of the drive laser power. The continuous line is a fit to Eq. (8). The inset shows the evolution of $S_{\delta\theta}(\omega)$ as the drive power is raised.

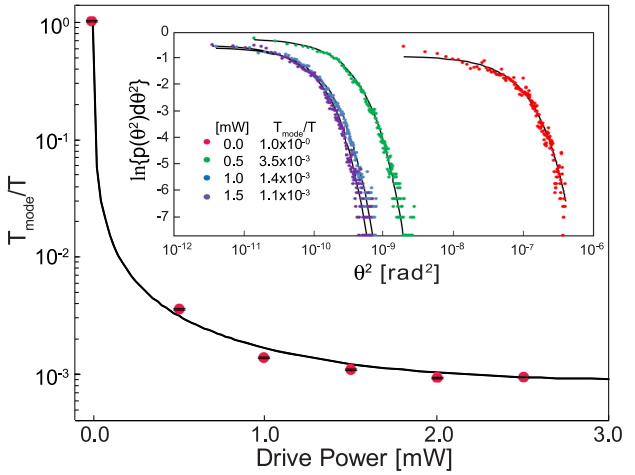

Fig. 3. Mode temperature from the measured statistical distribution of the mean-square angular fluctuation $\langle\delta\theta^2\rangle$ as a function of drive laser power. The continuous line is a fit to Eq. (8). The inset shows representative measured distributions $p(\theta^2)$ and their fits to Eq. (11). The fits would appear linear on semilogarithmic axes, but making the horizontal axis logarithmic as well facilitates the visualization of the reduction of $\langle\delta\theta^2\rangle$.

The whole experiment is placed atop a mechanically isolating optical table to improve stability. External vibrations mainly couple to the string modes of the ONF. However, we have observed mechanical coupling of the torsional modes to the environment from the turbomolecular pump. For this reason, we turn off the pump for the duration of the measurements, which is typically about 10 min. Small temperature instabilities in the laboratory can cause light polarization to drift in the hour timescale since the ONF is not polarization-maintaining. For this reason, we monitor all outputs of the BPD, searching for polarization drifts and correcting them when needed.

4. RESULTS

Figure 2 shows the ratio of the mode temperature T_{mode} to the ambient temperature, $T \approx 300$ K, as a function of drive power (feedback). The mode temperature is inferred from the integral of the out-of-loop angular spectral density $S_{\delta\theta}(\omega)$, and the solid line shows a fit to Eq. (8). The inset shows the evolution of $S_{\delta\theta}(\omega)$ as the drive power increases. The amplitude drops toward the noise floor, the width broadens, and the mean-square angular fluctuation $\langle\delta\theta^2\rangle$ given by the integral of $S_{\delta\theta}$ diminishes. Drive powers higher than 1.5 mW do not result in better cooling. Indeed, "squashing" [1,28] (not shown) appears in the in-loop signal as the g^2 term in Eq. (8) takes over, rendering the cooling less effective. The lowest mode temperature that we infer from these data is $T_{\mathrm{mode}}/T = 4.0(1) \times 10^{-3}$, corresponding to $T_{\mathrm{mode}} \approx 1.2$ K.

Figure 3 shows a complementary measurement of the mode temperature, made by using the spectrum analyzer as a combination of square-law detector and bandpass filter to infer the squared fluctuating amplitude $\delta\theta^2(t)$. Again, the measurements use out-of-loop data, and the solid line is a fit to Eq. (8). Representative statistics of $\delta\theta^2$ for time-series measurements of 10 s are shown in the inset, along with fits to the Boltzmann distribution given in Eq. (11). The limiting temperature that we observe here is $T_{\mathrm{mode}}/T = 1.11(1) \times 10^{-3}$, or $T_{\mathrm{mode}} \approx 330$ mK.

While we have followed the performance of the first torsional mode of the nanofiber carefully, the higher-order ones also show cooling. We believe the bandwidth of the feedback is sufficiently broad to have a direct effect, rather than other possible coupling mechanisms that we have left unexplored. Further, all high-order torsional modes show optomechanical coupling and can be cooled individually with the presented method. We also reproduce our results for different ONF radii.

5. DISCUSSION AND OUTLOOK

It is of interest to compare the degree of cooling we achieve to the expected limit given by Eq. (9) from the SNR. The noise floor is dominated by classical laser intensity noise and electronic (dark) noise, both of similar amplitudes for a 180 μW probe. We measure the contribution of both noise sources to the system by measuring the electronic voltage noise without the ONF, both with and without probe light striking the detectors. We refer the voltage noise back to effective angular noise by dividing it by the same calibration constant used to interpret the data with the ONF. We currently use commercial detector units operating near their maximum responsivity, corresponding to quantum efficiencies >90%. Upon coupling the probe into the fiber, the overall detection efficiency of the system should be greater than 80%. The overall SNR could be further improved by using lower-noise electronics and a shot-noise-limited probe laser.

The amplitude of the signal for the data set shown in Fig. 2 measured on resonance is $S_s = 4.50(9) \times 10^{-9}$ rad^2/Hz, while for the data set shown in Fig. 3 is $S_s = 2\langle\delta\theta^2\rangle/\Gamma = 3.90(3) \times 10^{-8}$ rad^2/Hz. The difference is due to systematic experimental variations typically observed. The nanofiber system is made from a nonpolarization-maintaining optical fiber, which causes the light polarization at the ONF to drift and imposes a technical challenge to set truly linearly polarized light at the ONF waist [35]. The differences in the signals from the data sets shown here highlight the role of the SNR in the cooling performance. The corresponding limiting mode temperature, from Eq. (9), is $T_{\mathrm{mode}}/T = 4.90(4) \times 10^{-3}$ and $T_{\mathrm{mode}}/T = 1.664(4) \times 10^{-3}$, respectively, in close agreement with the observed values. To increase the SNR, it would be desirable to enhance the mechanical transduction. Since the birefringence supplying the transduction in the ONF was an unintended artifact of the fabrication process, increasing it by a modification of the process seems plausible.

An independent study, performed in parallel to ours, shows similar results using electrodes for feedback-cooling an ONF torsional mode [36].

Once the detection quantum shot-noise limit is reached, one can apply standard techniques from the detection of squeezing. Further, it is possible to become less sensitive to the overall losses and efficiencies in propagation by applying conditional measurements [37]. Under those conditions, the field of quantum feedback opens new avenues on the platform [38,39]. In such a regime, one must address the effects of the back-action from the probe and the detection. On the one hand, the probe exerts torque on the ONF while sensing it, a common feature in many optomechanical systems [40]. Fluctuations in this torque will manifest themselves by inducing angular noise. We have varied the probe power by a factor of 5 and found no significant change in the SNR nor in the lowest achievable temperature, as the noise is dominated by classical intensity noise. This indicates that back-action from the probe is not a problem in the out-of-loop detection.

On the other hand, back-action effects from detection are already manifest in the squashing observed on the in-loop detection at the limit when the system achieves its lowest temperature. Previous studies in quantum optics have proposed using this to enhance signal-to-noise ratios in in-loop measurements [41]. Therefore, one could explore applying similar techniques to an optomechanical system limited by detection shot-noise, improving sensitivity to torque measurements in the nanofiber platform.

Beyond the optomechanical cooling capabilities of the platform, its high sensitivity to rotations makes ONFs a viable candidate for a torque sensor once systematic effects are controlled. The tensile strength of an ONF could allow its use as a torsional pendulum for precision force measurement [17]. Torsional modes also couple to external electric fields [25,36] presenting

a potential field sensor. The sensitivity of the platform is ultimately defined by the noise floor, S_{θ_n}, corresponding to a rotational sensitivity of $\approx 1.6 \times 10^{-7}$ rad$/\sqrt{\text{Hz}}$. The conversion from rotation to torque depends on the modulus of the angular displacement susceptibility, which on resonance is $\chi(\omega_0) = 1/\omega_0\gamma$. We thus obtain a torque sensitivity of $\approx 2.9 \times 10^{-26}$ N m Hz$^{-1/2}$, which is competitive with state-of-the-art rotational sensors [30]. The large scale of the system could allow for a larger interaction region of the sensor, improving the overall sensitivity and enabling measurements of quantum vacuum friction of polarizable objects near surfaces [30].

Since ONFs are known to be compatible with mK dilution refrigerators while guiding a few mW of optical power [42], ground-state cooling appears feasible. Indeed, at an ambient temperature of $T \approx 8$ mK, the mode temperature in Eq. (9) achievable with our current SNR yields a phonon occupation number $\langle n \rangle = (e^{-h\nu/k_B T_{\text{mode}}} - 1)^{-1} \approx 1$. Improvements to the SNR would allow starting from a higher ambient temperature, only limited by the necessary condition $Q\nu_m > k_B T/h$, which requires $T < 1.1$ K. In this regime, techniques more appropriate to assessing $\langle n \rangle$ than those employed here are available. In particular, the polarization rotation at ω_m induced by the nanofiber imparts phase modulation sidebands on the transmitted probe light at frequencies $\pm\omega_m$, in addition to modulating the differential intensity measured by the polarization analyzers shown in Fig. 1. A simple modification of our experimental apparatus as done earlier [26], beating the transmitted light with a local oscillator, would allow the sidebands to be readily measured in the rf domain. The ratio of the power in the sidebands is proportional to $\langle n \rangle/(1 + \langle n \rangle)$ [43], which differs from unity as the quantum regime is approached.

Ground-state cooling of massive objects has implications in quantum technologies [44] and quantum foundations and tests of gravitational effects in quantum theory [45,46]. For example, by preparing the mechanical state in a quantum superposition, one could test gravity-induced quantum collapse models [47], which benefit from using massive objects over large spatial extensions. In that regard, ONFs offer promise as candidates to study quantum torsional optomechanics of relatively massive (≈1 ng) and large-scale (≈1 cm size) objects.

6. CONCLUSION

In summary, we demonstrate optical feedback cooling of the fundamental torsional mode of a 5 mm long optical nanofiber, reducing the effective mode temperature by three orders of magnitude, reaching a mode temperature of ≈320 mK using optomechanical transduction in a cavityless system. The polarization of the guided light couples to the fiber via its intrinsic birefringence, enabling a sensitive probe of its rotation and a mechanism to optically apply torque for control purposes. We characterize the cooling in the frequency and time domains and find results that are near the limit imposed by the SNR. Finally, we discuss the possibilities of utilizing the platform as a torque sensor and suggest that reaching the quantum regime should be possible with a combination of cryogenic and optical feedback cooling.

Funding. National Key Research and Development Program of China (2022YFA1404201); FONDECYT (11200192); CONICYT-PAI (77190033); 111 Project (D18001); "1331 KSC", PCSIRT (IRT_17R70); Fundamental Research Program of Shanxi Province, China (20210302124537); National Natural Science Foundation of China (12034012, 12074231, 12274272, 61827824, 62105191).

Acknowledgment. We thank P. Zoller for his continuous interest. P. S. is a CIFAR Azrieli Global Scholar in the Quantum Information Science Program. This work was supported by the National Key Research and Development Program of China, the National Institute of Standards and Technology, USA, National Natural Science Foundation of China, Fundamental Research Program of Shanxi Province, "1331 KSC," PCSIRT, 111 Project from China, and FONDECYT and PAI projects from Chile.

Disclosures. The authors declare no conflicts of interest.

Data Availability. Data underlying the results presented in this paper are not publicly available at this time but may be obtained from the authors upon reasonable request.

REFERENCES

1. M. Aspelmeyer, T. J. Kippenberg, and F. Marquardt, "Cavity optomechanics," Rev. Mod. Phys. **86**, 1391–1452 (2014).
2. A. D. O'Connell, M. Hofheinz, M. Ansmann, R. C. Bialczak, M. Lenander, E. Lucero, M. Neeley, D. Sank, H. Wang, M. Weides, J. Wenner, J. M. Martinis, and A. N. Cleland, "Quantum ground state and single-phonon control of a mechanical resonator," Nature **464**, 697–703 (2010).
3. E. Verhagen, S. Deléglise, S. Weis, A. Schliesser, and T. J. Kippenberg, "Quantum-coherent coupling of a mechanical oscillator to an optical cavity mode," Nature **482**, 63–67 (2012).
4. J. Chan, T. P. M. Alegre, A. H. Safavi-Naeini, J. T. Hill, A. Krause, S. Gröblacher, M. Aspelmeyer, and O. Painter, "Laser cooling of a nanomechanical oscillator into its quantum ground state," Nature **478**, 89–92 (2011).
5. J. D. Teufel, T. Donner, D. Li, J. W. Harlow, M. S. Allman, K. Cicak, A. J. Sirois, J. D. Whittaker, K. W. Lehnert, and R. W. Simmonds, "Sideband cooling of micromechanical motion to the quantum ground state," Nature **475**, 359–363 (2011).
6. T. A. Palomaki, J. D. Teufel, R. W. Simmonds, and K. W. Lehnert, "Entangling mechanical motion with microwave fields," Science **342**, 710–713 (2013).
7. T. P. Purdy, R. W. Peterson, and C. A. Regal, "Observation of radiation pressure shot noise on a macroscopic object," Science **339**, 801–804 (2013).
8. A. H. Safavi-Naeini, S. Gröblacher, J. T. Hill, J. Chan, M. Aspelmeyer, and O. Painter, "Squeezed light from a silicon micromechanical resonator," Nature **500**, 185–189 (2013).
9. M. Rossi, D. Mason, J. Chen, Y. Tsaturyan, and A. Schliesser, "Measurement-based quantum control of mechanical motion," Nature **563**, 53–58 (2018).
10. U. Delić, M. Reisenbauer, K. Dare, D. Grass, V. Vuletić, N. Kiesel, and M. Aspelmeyer, "Cooling of a levitated nanoparticle to the motional quantum ground state," Science **367**, 892–895 (2020).
11. W. Marshall, C. Simon, R. Penrose, and D. Bouwmeester, "Towards quantum superpositions of a mirror," Phys. Rev. Lett. **91**, 130401 (2003).
12. C. Marletto and V. Vedral, "Gravitationally induced entanglement between two massive particles is sufficient evidence of quantum effects in gravity," Phys. Rev. Lett. **119**, 240402 (2017).

13. S. Bose, A. Mazumdar, G. W. Morley, H. Ulbricht, M. Toroš, M. Paternostro, A. A. Geraci, P. F. Barker, M. S. Kim, and G. Milburn, "Spin entanglement witness for quantum gravity," Phys. Rev. Lett. **119**, 240401 (2017).
14. J. Schmöle, M. Dragosits, H. Hepach, and M. Aspelmeyer, "A micromechanical proof-of-principle experiment for measuring the gravitational force of milligram masses," Classical Quantum Gravity **33**, 125031 (2016).
15. A. Al Balushi, W. Cong, and R. B. Mann, "Optomechanical quantum Cavendish experiment," Phys. Rev. A **98**, 043811 (2018).
16. Y. Liu, J. Mummery, J. Zhou, and M. A. Sillanpää, "Gravitational forces between nonclassical mechanical oscillators," Phys. Rev. Appl. **15**, 034004 (2021).
17. T. Westphal, H. Hepach, J. Pfaff, and M. Aspelmeyer, "Measurement of gravitational coupling between millimetre-sized masses," Nature **591**, 225–228 (2021).
18. A. Schliesser, O. Arcizet, R. Rivière, G. Anetsberger, and T. J. Kippenberg, "Resolved-sideband cooling and position measurement of a micromechanical oscillator close to the Heisenberg uncertainty limit," Nat. Phys. **5**, 509–514 (2009).
19. H. Shi and M. Bhattacharya, "Optomechanics based on angular momentum exchange between light and matter," J. Phys. B **49**, 153001 (2016).
20. D. Vitali, S. Mancini, L. Ribichini, and P. Tombesi, "Mirror quiescence and high-sensitivity position measurements with feedback," Phys. Rev. A **65**, 063803 (2002).
21. D. Kleckner and D. Bouwmeester, "Sub-kelvin optical cooling of a micromechanical resonator," Nature **444**, 75–78 (2006).
22. T. Corbitt, C. Wipf, T. Bodiya, D. Ottaway, D. Sigg, N. Smith, S. Whitcomb, and N. Mavalvala, "Optical dilution and feedback cooling of a gram-scale oscillator to 6.9 mK," Phys. Rev. Lett. **99**, 160801 (2007).
23. J. Gieseler, B. Deutsch, R. Quidant, and L. Novotny, "Subkelvin parametric feedback cooling of a laser-trapped nanoparticle," Phys. Rev. Lett. **109**, 103603 (2012).
24. L. Dania, D. S. Bykov, M. Knoll, P. Mestres, and T. E. Northup, "Optical and electrical feedback cooling of a silica nanoparticle levitated in a Paul trap," Phys. Rev. Res. **3**, 013018 (2021).
25. C. Wuttke, G. D. Cole, and A. Rauschenbeutel, "Optically active mechanical modes of tapered optical fibers," Phys. Rev. A **88**, 061801 (2013).
26. E. F. Fenton, A. Khan, P. Solano, L. A. Orozco, and F. K. Fatemi, "Spin-optomechanical coupling between light and a nanofiber torsional mode," Opt. Lett. **43**, 1534–1537 (2018).
27. D. Su, P. Solano, J. D. Wack, L. A. Orozco, and Y. Zhao, "Torsional optomechanical cooling of a nanofiber," Photon. Res. **10**, 601–609 (2022).
28. M. Poggio, C. L. Degen, H. J. Mamin, and D. Rugar, "Feedback cooling of a cantilever's fundamental mode below 5 mK," Phys. Rev. Lett. **99**, 017201 (2007).
29. T. W. Penny, A. Pontin, and P. F. Barker, "Performance and limits of feedback cooling methods for levitated oscillators: a direct comparison," Phys. Rev. A **104**, 023502 (2021).
30. J. Ahn, Z. Xu, J. Bang, P. Ju, X. Gao, and T. Li, "Ultrasensitive torque detection with an optically levitated nanorotor," Nat. Nanotechnol. **15**, 89–93 (2020).
31. D. Hümmer, P. Schneeweiss, A. Rauschenbeutel, and O. Romero-Isart, "Heating in nanophotonic traps for cold atoms," Phys. Rev. X **9**, 041034 (2019).
32. M. E. J. Friese, T. A. Nieminen, N. R. Heckenberg, and H. Rubinsztein-Dunlop, "Optical alignment and spinning of laser-trapped microscopic particles," Nature **394**, 348–350 (1998).
33. J. E. Hoffman, S. Ravets, J. A. Grover, P. Solano, P. R. Kordell, J. D. Wong-Campos, L. A. Orozco, and S. L. Rolston, "Ultrahigh transmission optical nanofibers," AIP Adv. **4**, 067124 (2014).
34. S. Ravets, J. E. Hoffman, L. A. Orozco, S. L. Rolston, G. Beadie, and F. K. Fatemi, "A low-loss photonic silica nanofiber for higher-order modes," Opt. Express **21**, 18325–18335 (2013).
35. M. Joos, A. Bramati, and Q. Glorieux, "Complete polarization control for a nanofiber waveguide using the scattering properties," Opt. Express **27**, 18818–18830 (2019).
36. F. Tebbenjohanns, J. Jia, M. Antesberger, A. S. Prasad, S. Pucher, A. Rauschenbeutel, J. Volz, and P. Schneeweiss, "Feedback-cooling the fundamental torsional mechanical mode of a tapered optical fiber to 30 mK," Phys. Rev. A **108**, L031101 (2023).
37. H. Carmichael, G. Foster, L. Orozco, J. Reiner, and P. Rice, "Chap. Intensity-field correlations of non-classical light," in *Progress in Optics* (Elsevier, 2004), Vol. **46**, pp. 355–403.
38. W. P. Smith, J. E. Reiner, L. A. Orozco, S. Kuhr, and H. M. Wiseman, "Capture and release of a conditional state of a cavity QED system by quantum feedback," Phys. Rev. Lett. **89**, 133601 (2002).
39. H. M. Wiseman and G. J. Milburn, *Quantum Measurement and Control* (Cambridge University, 2009).
40. T. J. Kippenberg and K. J. Vahala, "Cavity optomechanics: back-action at the mesoscale," Science **321**, 1172–1176 (2008).
41. H. M. Wiseman, "In-loop squeezing is like real squeezing to an in-loop atom," Phys. Rev. Lett. **81**, 3840–3843 (1998).
42. K. D. Voigt, J. B. Hertzberg, J. E. Hoffman, J. A. Grover, P. Solano, R. P. Budoyo, C. Ballard, J. Lee, J. R. Anderson, C. J. Lobb, L. A. Orozco, S. L. Rolston, and F. C. Wellstood, "Movable thin-film superconducting resonator coupled to a tapered optical microfiber at 15 mK," IEEE Trans. Appl. Supercond. **25**, 1700305 (2015).
43. F. Tebbenjohanns, M. Frimmer, V. Jain, D. Windey, and L. Novotny, "Motional sideband asymmetry of a nanoparticle optically levitated in free space," Phys. Rev. Lett. **124**, 013603 (2020).
44. S. Barzanjeh, A. Xuereb, S. Gröblacher, M. Paternostro, C. A. Regal, and E. M. Weig, "Optomechanics for quantum technologies," Nat. Phys. **18**, 15–24 (2022).
45. J. Millen and B. A. Stickler, "Quantum experiments with microscale particles," Contemp. Phys. **61**, 155–168 (2020).
46. D. C. Moore and A. A. Geraci, "Searching for new physics using optically levitated sensors," Quantum Sci. Technol. **6**, 014008 (2021).
47. A. Bassi, K. Lochan, S. Satin, T. P. Singh, and H. Ulbricht, "Models of wave-function collapse, underlying theories, and experimental tests," Rev. Mod. Phys. **85**, 471–527 (2013).